

Quantum thermodynamic processes: A control theory for machine cycles

Jan Birjukov¹, Thomas Jahnke², and Günter Mahler²

¹ Chair for Theoretical Physics and Applied Mathematics, Urals State Technical University, Mira 19, 620002 Jekaterinburg, Russia

² Institut für Theoretische Physik 1, Universität Stuttgart, Pfaffenwaldring 57, D-70550 Stuttgart, Germany

December 4, 2007

Abstract. The minimal set of thermodynamic control parameters consists of a statistical (thermal) and a mechanical one. These suffice to introduce all the pertinent thermodynamic variables; thermodynamic processes can then be defined as curves on this 2-dimensional control plane. Putting aside coherence we show that for a large class of quantum objects with discrete spectra and for the cycles considered the Carnot efficiency applies as a universal upper bound. In the dynamic (finite time) regime renormalized thermodynamic variables allow to include non-equilibrium phenomena in a systematic way. The machine function ceases to exist in the large speed limit; the way, in which this limit is reached, depends on the type of cycle used.

PACS. 05.30.-d Quantum statistical mechanics – 05.70.Ln Nonequilibrium and irreversible thermodynamics

1 Introduction

Physical systems can often be designed to implement a certain functionality. Well known examples include devices like sensors or logical elements underlying information processing. Here, much insight can be gained by restricting oneself to a kind of system theoretical approach, in which details of implementation are put aside. A recent example is quantum computation, in which a general theoretical framework allows to analyze fundamental limitations and possibilities [1].

Thermodynamics [2, 3, 4], in a sense, is a powerful control theory [3], with extremely widespread applications. One seeks general results independent of whether one is concerned with a classical gas, a magnetic material, or chemical reactions.

As a phenomenological theory thermodynamics cannot define its own limitations; however, it is usually taken to apply to large systems only (thermodynamic limit [4]).

Recently, it has been shown that thermodynamical properties emerge already for small quantum systems provided they are embedded in some appropriate environment [5]. As a consequence, the idea that a single small quantum object might well be described by means of thermodynamic concepts should no longer be considered self-contradictory. Nano-thermodynamics [6, 7] is becoming an emergent field that might be relevant in many areas ranging from nano-physics to molecular biology.

Deviations from thermodynamic equilibrium within such systems are just the logical next step. Examples include

transport scenarios [8] and thermodynamic processes (underlying machine functions). In the nano-regime various levels of descriptions are possible [9, 10, 11, 12, 13, 14, 15, 16, 17, 18], that can mainly be classified by the extent to which explicit quantum effects are being taken into account.

Typically, some driving is needed as a source of non-equilibrium. Time dependence may either be included by means of a classical driving system or by coupling to another full quantum mechanical subsystem [18]. The dynamics of the machine itself may or may not be allowed to show some quantum mechanical coherence. Anyway, in this context one should observe that for the operation of a thermodynamic machine the coupling to heat baths is essential, not just an unavoidable nuisance; decoherence [19] should thus be dominant.

In this paper we intend to address the problem of thermodynamic processes within a somewhat minimalistic and phenomenological model frame: We suggest to simply parametrize the spectrum and the state of a quantum system (cf. [10, 11, 20]) and consider the parameters so introduced as the external control. In the ideal case this is all we need to capture the essentials of thermodynamic machines, their possible cycles and efficiencies. This simple control model will then be extended to include an internal time scale (phenomenological relaxation time) to allow for non-equilibrium effects. This gives us a direct access to finite time thermodynamics [21, 11].

In doing so, we assume that this system theoretical scheme captures the main features of any concrete imple-

mentation, for which coherence [10] does not play a major role. While there have been speculations about dramatic differences between classical and quantum machinery [22], (even claiming violations of the second law), we come here to the opposite conclusion: Classical and quantum mechanical machines behave essentially identical – to an extent, which is almost unbelievable. In fact, this scale-invariance could hardly be expected, if one took it for granted that the pertinent (thermodynamic) concepts would, indeed, only apply in the thermodynamic limit of the system considered.

2 Model of Control

We consider a quantum system with discrete spectrum embedded in some environment. The impact of the environment on the system is taken to consist of two qualitatively different types, which may be called mechanical and statistical, respectively. Provided the weak coupling conditions are met (see, e.g., [5]), we assume that the mechanical influence comes into action through a parameter-dependent spectrum of the effective Hamiltonian, $\{E_i^{\text{eff}}(\gamma)\}_{i=1}^N$, where N is the number of levels. In order to introduce the influence of statistical type, we postulate the existence of an attractor state $\tilde{\rho}(\alpha)$, governed by a single parameter α .

We further demand the possibility to treat both parts of the control independently, i.e. that a change of the spectrum should not lead to a disturbance of the occupation numbers. This implies that the the mechanical influence should not disturb the ratio between any two transition frequencies, $\omega_{ij} = (E_i^{\text{eff}} - E_j^{\text{eff}})/\hbar$. This special requirement is satisfied by

$$E_i^{\text{eff}}(\gamma) = g(\gamma) \cdot \epsilon_i, \quad (1)$$

where g is some monotonous function, and $\{\epsilon_i\}_{i=1}^N$ are to be regarded as a set of characteristic constants. As a pertinent example one could take a spin in magnetic field $B \approx \gamma$, so that $g(\gamma) = \gamma$. Another possible choice, $g(\gamma) = \gamma^{-2}$, was motivated by the quantum particle in a box, supposing the box width $L \approx \gamma$ to be adjustable. (In the 3-dimensional case, volume $V = L^3 \approx \gamma$ we would take $g(\gamma) = \gamma^{-2/3}$.)

We further assume that our quantum system always stays in a mixed state determined by the diagonal elements of its density matrix ρ in the respective energy representation, $\{p_i = \rho_{ii}\}_{i=1}^N$. If the eigenbasis is not invariant under the mechanical influence, this condition may be enforced by rapid decoherence (time scale τ_{dec}). Pure decoherence has no influence on the energy balance. Thus ρ and H^{eff} commute, making ρ stationary, i.e. excluding any coherence as well as any autonomous Schrödinger-dynamics.

The attractor state postulated above is assumed to be a member of this class of diagonal states and stable in the sense that whenever the actual distribution p_i differs from $\tilde{p}_i(\alpha)$, this deviation will decay on a time scale $\tau_R \gg \tau_{dec}$ according to

$$\dot{p}_i = -\tau_R^{-1}(p_i - \tilde{p}_i(\alpha)), \quad (2)$$

(relaxation time approximation).

Note that for τ_R small compared with the characteristic time of enforced α -parameter alterations, one gets

$$p_i = \tilde{p}_i(\alpha) \quad (3)$$

at all times, i.e. the so-called quasi-static limit [3].

3 Quasi-static limit

The quasi-static limit plays a fundamental role in standard thermodynamics. In the nano-domain, to be sure, this limit faces principle limitations: as all length scales shrink, also the possibilities of thermal isolation become severely constrained (cf. [23]). This means, e.g., that the interaction with baths of different temperatures may no longer be assumed to be switched on and off at will. Leakage becomes unavoidable [12,13,18]. This aspect will presently be excluded, as are any implementation issues.

Here the quasi-static limit will be taken to specify an important reference scenario: the limit of perfect control over a quantum system. Both the spectrum (1) and the energy distribution (3) are completely specified by γ and α taken to be external control parameters. Hence, as long as the thermodynamic quantities are properly defined, one can consider an arbitrary point in the (α, γ) -plane as a thermodynamic state implemented on the system under consideration.

3.1 Thermodynamic quantities

As follows from the foregoing, in the quasi-static limit one can define for the system's state corresponding to a certain point on the (α, γ) -plane the entropy S and the internal energy U [4]:

$$S(\alpha) := - \sum \ln \tilde{p}_i(\alpha) \cdot \tilde{p}_i(\alpha), \quad (4)$$

$$U(\alpha, \gamma) := g(\gamma) \sum \epsilon_i \cdot \tilde{p}_i(\alpha); \quad (5)$$

From (4) we observe, taking into account the normalization condition for $\{\tilde{p}_i(\alpha)\}_{i=1}^N$, that

$$\frac{dS}{d\alpha} = - \sum \ln \tilde{p}_i \left(\frac{d\tilde{p}_i}{d\alpha} \right). \quad (6)$$

In order to introduce the notion of temperature, we employ the formal definition [3,4], as the conjugate variable to the entropy S :

$$T := \left(\frac{\partial U}{\partial S} \right)_\gamma = \left(\frac{\partial U}{\partial \alpha} \right)_\gamma \left(\frac{dS}{d\alpha} \right)^{-1}. \quad (7)$$

Together with (5) and (6) one gets

$$T(\alpha, \gamma) = -g(\gamma) \frac{\sum \epsilon_i (d\tilde{p}_i/d\alpha)}{\sum \ln \tilde{p}_i (d\tilde{p}_i/d\alpha)} := g(\gamma) \Theta(\alpha)^{-1}. \quad (8)$$

We introduce, as well, the conjugate variable to γ :

$$P := - \left(\frac{\partial U}{\partial \gamma} \right)_\alpha \quad (9)$$

or, explicitly

$$P(\alpha, \gamma) = - \frac{dg}{d\gamma} \sum \epsilon_i \tilde{p}_i := \frac{dg}{d\gamma} \Pi(\alpha)^{-1} \quad (10)$$

For a classical gas with $\gamma = V$ (volume), P would be the conventional pressure.

Consider now the total differential of the internal energy (5) as a function of these control parameters [9]:

$$dU(\alpha, \gamma) = \left(\frac{\partial U}{\partial \alpha} \right)_\gamma d\alpha + \left(\frac{\partial U}{\partial \gamma} \right)_\alpha d\gamma. \quad (11)$$

Based on (7) we introduce the infinitesimal increment of heat, $\bar{d}Q = TdS$:

$$\bar{d}Q(\alpha, \gamma) := \left(\frac{\partial U}{\partial \alpha} \right)_\gamma d\alpha = g(\gamma) \sum \epsilon_i \left(\frac{d\tilde{p}_i}{d\alpha} \right) d\alpha. \quad (12)$$

As to the second term in (11), its meaning is the internal energy increment under constant α , in fact under constant entropy, cf. (4). It allows us to consider this term as work:

$$\bar{d}W(\alpha, \gamma) := \left(\frac{\partial U}{\partial \gamma} \right)_\alpha d\gamma = \frac{dg}{d\gamma} \sum \epsilon_i \tilde{p}_i d\gamma. \quad (13)$$

All those thermodynamic quantities defined via partial derivatives are connected with a specific process in the control plane (a line), not just a state (a point). While there can be no operators underlying these classical quantities they can, nevertheless, be defined for any appropriately embedded quantum system.

3.2 Specific processes

A process in the control plane is a sequence of states each characterized by some α, γ . It can thus be visualized as a curve in this control plane. Such a curve, in turn, can be defined by some constraint on the accessible values of control parameter pairs, $f(\alpha, \gamma) = \mathbf{const}$.

A comment might be in order here: It should be clear that only a limited subclass of such imaginable curves could actually be realized by means of any concrete implementation. This does not invalidate the present general concept, though. We do not have to assume that α and γ can freely be changed at will. We only need the possibility to realize some cycle in control space. Whether or not this cycle will come close to one of the ideal cycles to be discussed below, is not that important. Essentially we encounter the same situation within the classical regime: For a concrete device the class of possible cycles is more or less restricted.

The simplest examples for processes are *isentropes* and *isochores*, here identified with $\alpha = \mathbf{const}$ and $\gamma = \mathbf{const}$,

respectively. It is noteworthy that along an isentrope the temperature (8) is directly proportional to $g(\gamma)$. With $g(\gamma) = 1/\gamma$, for example, $T(\alpha, \gamma)$ will decrease with increasing γ :

$$T \approx \frac{1}{\gamma} \quad (14)$$

This is what happens for photons in a cavity of size $\gamma = L$, a phenomenon known also from the photon temperature reduction in our expanding universe (cosmic microwave background [24]). Another pertinent example is adiabatic demagnetization (magnetic cooling), with $g(\gamma) = \gamma \approx B$ and $T \approx \gamma$.

Based on (8), the definition of an *isothermal* process is straight forward: $T(\alpha, \gamma) = \mathbf{const}$ ($= T$). This constraint can be cast into the convenient form:

$$g(\gamma) = T \cdot \Theta(\alpha), \quad (15)$$

In (15) T plays the role of a scale factor: The shape of every isotherm is the same, depending eventually on the chosen form for $g(\gamma)$ and the one-parameter family of distributions, $\{\tilde{p}_i(\alpha)\}_{i=1}^N$, the attractor.

If, as a particular choice, one takes the *canonical attractor*:

$$\tilde{p}_i(\alpha) = Z_{can}^{-1} e^{-\alpha \epsilon_i}, \quad Z_{can} = \sum e^{-\alpha \epsilon_i}; \quad (16)$$

one finds

$$\Theta_{can}(\alpha) = \alpha. \quad (17)$$

With $g(\gamma) = \gamma$ the isotherms (15) will now be just straight lines in the control plane, $\gamma = \alpha T$ at constant T . With $g(\gamma) = \gamma^{-2}$ one would get $\gamma = 1/\sqrt{\alpha T}$, a sort of hyperbolae (see Fig. 1 and Fig. 2).

Finally, an effective *isobaric* process can be defined based on (10): $P(\alpha, \gamma) = \mathbf{const}$ ($= P$), i.e.

$$\frac{dg}{d\gamma} = P \cdot \Pi(\alpha), \quad (18)$$

In this case, P plays the role of a scale factor.

Assuming $g(\gamma) = \gamma^k$, isobars are described by

$$\gamma = \left(\frac{1}{k} P \cdot \Pi(\alpha) \right)^{\frac{1}{k-1}} \quad (19)$$

on the (α, γ) -plane. For example, isobars for a particle in a box ($g(\gamma) = \gamma^{-2}$) are given by

$$\gamma = \left(\frac{2 \sum \epsilon_i \tilde{p}_i(\alpha)}{P} \right)^{\frac{1}{3}}. \quad (20)$$

3.3 Heat and work

Bearing in mind the forthcoming analysis of various thermodynamic cycles, which underly heat engines or heat pumps operation, we consider the heat- and work-production

along the specific processes. Integrating (12) and (13), one gets for the canonical isotherms $g(\gamma) = T \cdot \alpha$:

$$Q_{\mathcal{T}} = T \sum \epsilon_i \int \alpha d\tilde{p}_i(\alpha) < 0; \quad (21a)$$

$$W_{\mathcal{T}} = T \sum \epsilon_i \int \tilde{p}_i(\alpha) d\alpha; \quad (21b)$$

for the isentropes $\alpha = \text{const}$:

$$Q_S = 0; \quad (22a)$$

$$W_S = \Delta g(\gamma) \sum \epsilon_i \tilde{p}_i(\alpha); \quad (22b)$$

and for the isochores $\gamma = \text{const}$:

$$Q_{\gamma} = g(\gamma) \sum \epsilon_i \Delta \tilde{p}_i(\alpha) < 0; \quad (23a)$$

$$W_{\gamma} = 0; \quad (23b)$$

where Δ denotes the corresponding increment along the process line.

The negative sign for the heat flows $Q_{\mathcal{T}}$ and Q_{γ} is proven in Appendix B for the case of the canonical attractor (16); the corresponding increments of α are supposed here to be positive. Such general sign statements cannot be proven for the work inputs $W_{\mathcal{T},S}$, as their sign depends, together with the rest, on the particular choice of $\{\epsilon_i\}_{i=1}^N$.

3.4 Carnot cycle

Provided $\Theta(\alpha)$ exists, it is always possible to compose a closed path in the (α, γ) -plane from two isentropes and two isotherms – thus leading to a conventional Carnot cycle.

All the pertinent thermodynamic quantities, such as entropy (4), internal energy (5), temperature (8), heat (12) and work (13) are defined in the quasi-static limit in such a way, that Eq. (11) turns into the Gibbsian fundamental form:

$$dU = TdS + \delta W, \quad (24)$$

irrespective of $g(\gamma)$ or the chosen kind of attractor (3). Work per cycle ($\Delta U = 0$) can thus be obtained, as usual, from

$$W = - \oint TdS \quad (25)$$

In the case of heat engine performance, thermodynamic efficiency is defined as the ratio $W/Q_{\mathcal{T}_h}$, where W is the total work output per cycle and $Q_{\mathcal{T}_h}$ is the heat input during the isothermal stage at $T = T_h > T_c$. Note that because of the cyclic operation, $Q_{\mathcal{T}_c} + Q_{\mathcal{T}_h} = W$. As usual, $Q_{\mathcal{T}_c} < 0$ is supposed to be discarded, i.e. cannot be re-used.

The validity of the Gibbsian fundamental form immediately leads to the Carnot efficiency [3]

$$\eta^c = 1 - \frac{T_c}{T_h}, \quad (26)$$

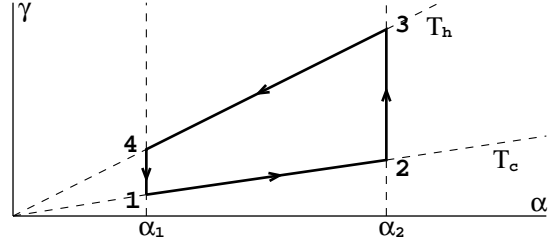


Fig. 1. Carnot's cycle on the (α, γ) -plane associated with the canonical attractor (16) and $g(\gamma) = \gamma$. It is composed by segments of isentropes $\alpha = \alpha_{1,2}$ and isotherms $\gamma = \alpha T_{c,h}$; ($T_h > T_c$). Arrows correspond to heat-engine performance.

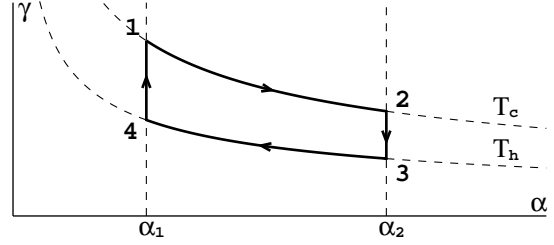


Fig. 2. As Fig. 1, but for $g(\gamma) = \gamma^{-2}$. The Carnot cycle is composed by segments of isentropes $\alpha = \alpha_{1,2}$ and isotherms $\gamma = 1/\sqrt{\alpha T_{c,h}}$; ($T_h > T_c$). Arrows correspond to heat-engine performance.

for any heat-engine cycle of Carnot's kind in the (α, γ) -plane with assigned temperatures $T_c < T_h$ for the isotherms (15), independent of details of the implementation. The Carnot efficiency as a limiting fundamental value does not even require thermal states, only the implementation of a 2-parameter control, as stated. The temperatures T_c, T_h would then only have a formal meaning, though. This is, in some sense, a generalization of the well-known universality established in conventional macroscopic thermodynamics.

In order to present an illustrative example, we explore the case of the canonical attractor (16). The corresponding Carnot cycles are sketched in Fig. 1 and Fig. 2.

According to (21a), for the heat-engine performance one must run the cycle in Fig. 1 anticlockwise, while the cycle in Fig. 2 clockwise: These directions correspond to heat input for the high- and heat output for the low-temperature isothermal stage, respectively. Treating both cycles stepwise based on (21) and (22), one explicitly gets the Carnot efficiency (26), as expected.

Two examples for other possible choices of the attractor type are given in Appendix A. These examples illustrate the fact that the shape of the Carnot cycle in control space depends on the underlying attractor, leading, though, in the quasi-static limit to the same form, when mapped on the (S, T) -space (Fig. 4). Also the efficiency is always given by the Carnot value; in this sense, one cannot win anything by trying to implement exotic distribution functions.

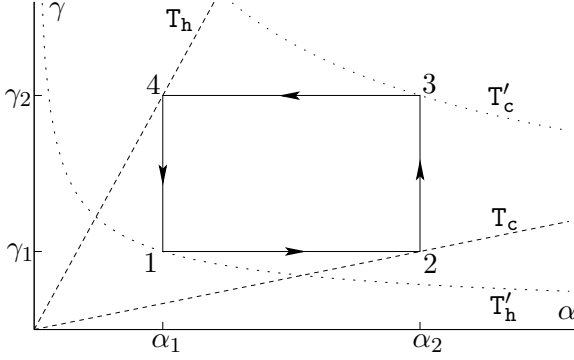


Fig. 3. Otto cycle on the (α, γ) -plane. The isentropes are given by $\alpha = \text{const}$ and the isochors by $\gamma = \text{const}$. The dashed lines are canonical isotherms with the highest and lowest temperature of the cycle for $g(\gamma) = \gamma$, while the dotted ones hold for $g(\gamma) = \gamma^{-2}$.

3.5 Otto cycle

As is well-known, the universality as is found for the Carnot cycle does not carry over to other cycle types. This means that the resulting efficiencies $\eta \leq \eta^c$ would then depend on the actual control functions $g(\gamma)$ and $\tilde{p}_i(\alpha)$.

The Otto cycle is in some sense the most fundamental quantum thermodynamic cycle: On the isentropes, there is only a change of the spectrum while on the isochors only the occupation numbers are changing. Most of the theoretically discussed quantum thermodynamic engines, in effect, are realized as Otto cycles [10, 16, 25].

Fig. 3 shows the Otto cycle on the (α, γ) -plane. As the Carnot cycle discussed above, this cycle must be run anticlockwise or clockwise, depending on the choice of $g(\gamma)$, in order to get the heat-engine performance.

If the function $g(\gamma)$ is increasing, (22) and (23) lead to the efficiency:

$$\eta^{\mathcal{O}} = 1 - \frac{g(\gamma_1)}{g(\gamma_2)}, \quad (27)$$

For a 2-level system, one gets, identifying

$$\Delta(\gamma) = g(\gamma)(\epsilon_2 - \epsilon_1) \quad (28)$$

the well-known result [26]

$$\eta = 1 - \frac{\Delta(\gamma_1)}{\Delta(\gamma_2)} \quad (29)$$

Which is often mistaken as representing the Carnot efficiency [27].

With decreasing $g(\gamma)$ one must run the cycle clockwise to get a heat-engine. The efficiency is then given by

$$\eta'^{\mathcal{O}} = 1 - \frac{g(\gamma_2)}{g(\gamma_1)}, \quad (30)$$

In any case, the efficiency only depends on the relative compression, just like for the classical Otto cycle [2].

To compare these results with the efficiency of the Carnot cycle, we use (15) and (17) to get

$$\eta^{\mathcal{O}} = 1 - \frac{T_c \alpha_2}{T_h \alpha_1} \quad (31a)$$

$$\eta'^{\mathcal{O}} = 1 - \frac{T'_c \alpha_2}{T'_h \alpha_1} \quad (31b)$$

where T_c (T'_c) is the lowest temperature and T_h (T'_h) the highest temperature along the cycle. As shown in Fig. 3, T_c is reached at point 2 and T_h at point 4 for increasing $g(\gamma)$, whereas for decreasing $g(\gamma)$ T'_c is reached at point 3 and T'_h at point 1 (cf. [10]). As one can see, the efficiency of the Otto cycle remains below the Carnot's value. Formally, the Carnot efficiency is reached for $\alpha_2 = \alpha_1$, when the total work output of the machine vanishes (cf. [16]).

In the following we shall give two examples of spectral control:

3.5.1 Example: Spin in the magnetic field

For a spin in the magnetic field B , $E_i \propto B$ holds. Identifying the control parameter γ with B , we have

$$g(\gamma) = \gamma \quad (32)$$

and therefore the efficiency (27) simply reads

$$\eta_{\text{spin}}^{\mathcal{O}} = 1 - \frac{\gamma_1}{\gamma_2}, \quad (33)$$

3.5.2 Example: Particle in a box

We now consider a particle in a box of length L [22]. The energy levels are then given by $E_i \propto 1/L^2$. Thus this length L can be used to control the spectrum. Identifying $\gamma \equiv L$ we have:

$$g(\gamma) = \frac{1}{\gamma^2} \quad (34)$$

Because $g(\gamma)$ is decreasing here, we have to take (30) as the efficiency:

$$\eta_{\text{box}}^{\mathcal{O}} = 1 - \left(\frac{\gamma_1}{\gamma_2} \right)^2 \quad (35)$$

4 Non-Equilibrium

So far there has been no explicit consideration of dynamical features – as is typical for idealized thermodynamic modeling. We now focus on the thermodynamic quantities introduced in Sec. 3, when one allows for deviations of the momentary state from the enforced attractor state. This would come about if the pertinent attractor state was changing too fast (in terms of α) for the actual state to follow immediately.

As a result, the probabilities p_i no longer depend just on the momentary control $\alpha(t)$ as in the quasi-static limit (3); they also become dependent on their past history. Formally, such a non-equilibrium distribution can always be written as

$$p_i(\alpha, \Delta p_i) = \tilde{p}_i + \Delta p_i \quad (36)$$

where the additional parameters Δp_i are due to the dynamical response of the system and thus not directly under our control. If we stopped to change α and waited long enough, all the Δp_i should disappear, according to (2).

The internal energy and entropy can be defined for any state (we indicate non-equilibrium by an asterisk), $U^* = U^*(\alpha, \gamma, \Delta p_i)$, $S^* = S^*(\alpha, \Delta p_i)$ just by replacing \tilde{p}_i in (5) and (4) with p_i , and thus

$$dU^* = \left(\frac{\partial U^*}{\partial \gamma} \right)_{\alpha, \Delta p_i} d\gamma + \left(\frac{\partial U^*}{\partial \alpha} \right)_{\gamma, \Delta p_i} d\alpha + \bar{d}M^*, \quad (37)$$

where

$$\begin{aligned} \bar{d}M^* &= \sum \left(\frac{\partial U^*}{\partial \Delta p_i} \right)_{\gamma, \alpha} d(\Delta p_i) \\ &= g(\gamma) \sum \epsilon_i d\Delta p_i \end{aligned} \quad (38)$$

specifies the non-equilibrium contribution. We define the renormalized work as

$$\begin{aligned} \bar{d}W^* &= \left(\frac{\partial U^*}{\partial \gamma} \right)_{\alpha, \Delta p_i} d\gamma \\ &= \frac{dg}{d\gamma} \sum \epsilon_i p_i d\gamma \end{aligned} \quad (39)$$

and the heat as

$$\begin{aligned} \bar{d}Q^* &= \left(\frac{\partial U^*}{\partial \alpha} \right)_{\gamma, \Delta p_i} d\alpha + \bar{d}M^* \\ &= g(\gamma) \sum \epsilon_i \left(\frac{d\tilde{p}_i}{d\alpha} d\alpha + d(\Delta p_i) \right) \\ &= g(\gamma) \sum \epsilon_i dp_i \end{aligned} \quad (40)$$

The renormalized temperature T^* will be taken to remain a control variable asking for the response of U^* to a change of α (for given Δp_i)

$$T^*(\alpha, \gamma, \Delta p_i) = \left(\frac{\partial U^*}{\partial \alpha} \right)_{\gamma, \Delta p_i} \left(\frac{\partial S^*}{\partial \alpha} \right)_{\Delta p_i}^{-1}. \quad (41)$$

Because of

$$dS^* = \left(\frac{\partial S^*}{\partial \alpha} \right)_{\Delta p_i} d\alpha + \sum \left(\frac{\partial S^*}{\partial \Delta p_i} \right)_{\alpha} d(\Delta p_i) \quad (42)$$

the heat can alternatively be written as

$$\begin{aligned} \bar{d}Q^* &= T^* dS^* - T^* \sum \left(\frac{\partial S^*}{\partial \Delta p_i} \right)_{\alpha} d(\Delta p_i) + \bar{d}M^* \\ &= T^* dS^* - \bar{d}Q_{\text{diss}}^* \end{aligned} \quad (43)$$

with introducing the heat due to ‘‘dissipated work’’ [28]

$$\begin{aligned} \bar{d}Q_{\text{diss}}^* &= T^* \sum \left(\frac{\partial S^*}{\partial \Delta p_i} \right)_{\alpha} d(\Delta p_i) - \bar{d}M^* \\ &= - \sum [T^* \ln p_i + g(\gamma) \epsilon_i] d\Delta p_i. \end{aligned} \quad (44)$$

Heat is thus split into two terms, $T^* dS^*$ and $\bar{d}Q_{\text{diss}}^*$. With $\bar{d}Q_{\text{diss}}^* \geq 0$ eq. (43) defines the second law as stated by Clausius [28]:

$$\bar{d}Q^* \leq T^* dS^* \quad (45)$$

In the quasi-static limit Δp_i and thus $\bar{d}Q_{\text{diss}}^*$ is zero, and the equality sign holds in (45). $\bar{d}Q_{\text{diss}}^*$ is identically zero also for a 2-level system; this underlines the special character of this model. Instead of (25) the work per cycle is now given by

$$\Delta W^* = - \left(\oint T^* dS^* - \oint \bar{d}Q_{\text{diss}}^* \right) \quad (46)$$

We note that for a concrete process history, the Δp_i can be shown to become a function of the momentary α value, too. In the following we assume the time-dependence of the control parameter $\alpha(t)$ to be:

$$\alpha = \alpha_0 + vt, \quad (47)$$

where v may be positive or negative. Of course, there are other possible choices, indicating that more details of the control may become important.

With the attractor $\{\tilde{p}_i(\alpha)\}_{i=1}^N$ being driven by this $\alpha(t)$ according to (47), the relaxation equations (2) take the form:

$$(dp_i/d\alpha) = -(v\tau_R)^{-1}(p_i - \tilde{p}_i(\alpha)) \quad (48)$$

and yield the solutions:

$$p_i = p_i^{(0)} e^{-\frac{\alpha - \alpha_0}{v\tau_R}} + (v\tau_R)^{-1} \int_{\alpha_0}^{\alpha} \tilde{p}_i(\alpha') e^{-\frac{\alpha - \alpha'}{v\tau_R}} d\alpha'. \quad (49)$$

This means that the p_i could still be considered to be an explicit function of α only as soon as the initial values p_i^0 and α_0 are specified by the given process history.

In order to realize a cyclic process in the (α, γ) -control plane, we have to assign $\alpha(t)$ for both running directions between the turning points α_1 and α_2 . We allow for different driving speeds, namely:

$$\alpha_{1 \rightarrow 2}(t) = \alpha_1 + \kappa t; \quad \alpha_{2 \rightarrow 1}(t) = \alpha_2 - \lambda \kappa t, \quad (50)$$

with $\kappa, \lambda > 0$.

Considering (49) with $v = \kappa$ and $v = -\lambda\kappa$, respectively, one comes up with the following distributions at the turning points in the stationary cyclic regime:

$$\begin{aligned} p_i^{(1)} &= \left(e^{\frac{\Delta\alpha}{\lambda\kappa\tau_R}} - e^{-\frac{\Delta\alpha}{\kappa\tau_R}} \right)^{-1} \cdot (\kappa\tau_R)^{-1} \\ &\times \int_{\alpha_1}^{\alpha_2} \tilde{p}_i(\alpha') \left(e^{-\frac{\alpha_2 - \alpha'}{\kappa\tau_R}} + \frac{1}{\lambda} e^{\frac{\alpha_2 - \alpha'}{\kappa\tau_R}} \right) d\alpha'; \end{aligned} \quad (51a)$$

$$\begin{aligned} p_i^{(2)} &= \left(e^{\frac{\Delta\alpha}{\kappa\tau_R}} - e^{-\frac{\Delta\alpha}{\lambda\kappa\tau_R}} \right)^{-1} \cdot (\kappa\tau_R)^{-1} \\ &\times \int_{\alpha_1}^{\alpha_2} \tilde{p}_i(\alpha') \left(e^{\frac{\alpha' - \alpha_1}{\kappa\tau_R}} + \frac{1}{\lambda} e^{-\frac{\alpha' - \alpha_1}{\lambda\kappa\tau_R}} \right) d\alpha'; \end{aligned} \quad (51b)$$

5 Beyond the quasi-static limit

5.1 Renormalized process temperature

The renormalized temperature (41) now reads, observing (36)

$$T^* = -g(\gamma) \frac{\sum \epsilon_i (d\tilde{p}_i/d\alpha)}{\sum \ln p_i (d\tilde{p}_i/d\alpha)}. \quad (52)$$

The quantity T^* , determined in this way, we shall call *process temperature*.

In order to understand what happens with the process temperature along non-isentropic curves in the (α, γ) -plane, we consider the asymptote under very slow driving, $(v\tau_R/\Delta\alpha) \ll 1$, when the following expansion holds (see App. C):

$$p_i = \tilde{p}_i(\alpha) - v\tau_R \frac{d\tilde{p}_i}{d\alpha} + o\left[\frac{v\tau_R}{\Delta\alpha}\right], \quad (53)$$

where $\Delta\alpha$ denotes the increment of α in the course of the process. Inserting this expansion into (52) and keeping terms up to first order in $(v\tau_R/\Delta\alpha)$, one gets:

$$T^* = T(\alpha, \gamma) \left(1 + v\tau_R \frac{\sum (1/\tilde{p}_i)(d\tilde{p}_i/d\alpha)^2}{\sum \ln \tilde{p}_i (d\tilde{p}_i/d\alpha)} \right) + o\left[\frac{v\tau_R}{\Delta\alpha}\right], \quad (54)$$

observing as well the definition (8) for the temperature $T(\alpha, \gamma)$ in the quasi-static limit.

Of course, any chosen process line $f(\alpha, \gamma) = \text{const}$ implies a certain relationship between γ and α . In the canonical case (17) and when the process $\alpha(t)$ is taken to run along the line (15), which would be an isotherm with $T(\alpha, \gamma) = T$ in the quasi-static limit, Eq. (54) reduces to:

$$T^*(\alpha) = T \left(1 + \frac{v\tau_R}{\alpha} \right) + o\left[\frac{v\tau_R}{\Delta\alpha}\right], \quad (55)$$

For a Carnot machine cycle (Fig. 1 and Fig. 2) this means, compared with the quasi-static limit, that the dynamically renormalized process temperature is increased for increasing α ($v > 0$, contact with a heat sink) and decreased for decreasing α ($v < 0$, heat source). This is a non-equilibrium phenomenon; T^* is no longer constant even along the originally isothermal control process (Fig. 4 cf. [11]). Temperature shifts like those following from (55) have *ad hoc* been introduced in Curzon and Ahlborn's finite time analysis of the heat engine efficiency [21]. Already at $v\tau_R \approx 1$, however, the ST loop proper is dominated by counteracting non-equilibrium excursions.

5.2 Renormalized heat and work

Consider the renormalized heat- and work-production along those specific processes underlying Carnot and Otto cycles. One has to integrate now (40) and (39) along the corresponding lines in the (α, γ) -plane. In the case of the canonical isotherm $g(\gamma) = \alpha T$ this leads to the integrals

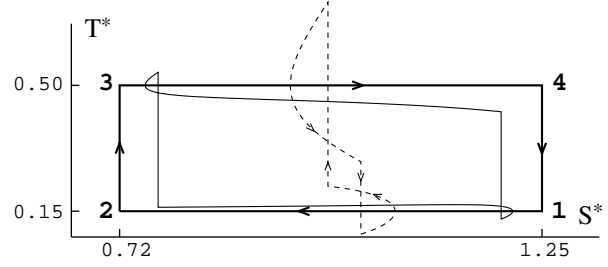


Fig. 4. Carnot cycle in the (S^*, T^*) -plane. Both cycles from Fig. 1 and Fig. 2 look similar here. The rectangle denotes the perfect Carnot cycle in the quasi-static limit $v\tau_R = 0$. The solid line corresponds to a steady cyclic regime at $v\tau_R = 0.09$; the dashed one – at $v\tau_R = 0.9$. This is a result of numerical simulations in accordance with $S^* := -\sum \ln p_i \cdot p_i$ and (52), with p_i under relaxation (49). The set of constants $\{\epsilon_i\}_{i=1}^N$ is chosen here to be $\{-3/2; -1/2; 1/2; 3/2\}$.

$\int_{\alpha_0}^{\alpha} \alpha' dp_i$ and $\int_{\alpha_0}^{\alpha} p_i d\alpha'$, with the probabilities p_i under relaxation as given by (49). The latter is readily achievable directly from the relaxation equation (48):

$$\int_{\alpha_0}^{\alpha} p_i d\alpha' = \int_{\alpha_0}^{\alpha} \tilde{p}_i(\alpha') d\alpha' - v\tau_R (p_i - p_i^{(0)}), \quad (56)$$

immediately followed by:

$$\int_{\alpha_0}^{\alpha} \alpha' dp_i = \int_{\alpha_0}^{\alpha} \alpha' d\tilde{p}_i(\alpha') + \alpha (p_i - \tilde{p}_i(\alpha)) - \alpha_0 (p_i^{(0)} - \tilde{p}_i(\alpha_0)) + v\tau_R (p_i - p_i^{(0)}). \quad (57)$$

Renormalized isothermal heat and work are thus in the canonical case:

$$\begin{aligned} Q_{\mathcal{T}}^* &= Q_{\mathcal{T}} + q + q' + q'', \\ q &:= v\tau_R T \sum \epsilon_i (p_i - p_i^{(0)}), \\ q' &:= -\alpha_0 T \sum \epsilon_i (p_i^{(0)} - \tilde{p}_i(\alpha_0)), \\ q'' &:= \alpha T \sum \epsilon_i (p_i - \tilde{p}_i(\alpha)); \end{aligned} \quad (58a)$$

$$\begin{aligned} W_{\mathcal{T}}^* &= W_{\mathcal{T}} + w, \\ w &:= -v\tau_R T \sum \epsilon_i (p_i - p_i^{(0)}) = -q; \end{aligned} \quad (58b)$$

Again, the respective renormalized quantities are denoted by an asterisk, while the heat and work in the quasi-static limit (right hand side) are defined according to (21).

Integration along the isentropic line $\alpha = \text{const}$ yields zero for the heat and $\Delta g \sum \epsilon_i p_i^{(0)}$ for the work, due to the conservation of the respective distribution — the results are similar to those obtained in the quasi-static limit (22):

$$Q_S^* = 0; \quad (59a)$$

$$\begin{aligned} W_S^* &= W_S + w', \\ w' &:= \Delta g(\gamma) \sum \epsilon_i (p_i^{(0)} - \tilde{p}_i(\alpha_0)); \end{aligned} \quad (59b)$$

Finally, for the isochores $\gamma = \text{const}$ one gets:

$$\begin{aligned} Q_\gamma^* &= Q_\gamma + \tilde{q} + \tilde{\tilde{q}}, \\ \tilde{q} &:= -g(\gamma) \sum \epsilon_i \left(p_i^{(0)} - \tilde{p}_i(\alpha_0) \right), \\ \tilde{\tilde{q}} &:= g(\gamma) \sum \epsilon_i \left(p_i - \tilde{p}_i(\alpha) \right); \end{aligned} \quad (60a)$$

$$W_\gamma^* = 0; \quad (60b)$$

where Q_γ^* , as well as W_γ^* before, is formally expressed through its quasi-static value.

5.3 Finite-time Carnot cycle

We turn now to the Carnot cycle shown in Fig. 1 and Fig. 2 run according to (50) with the speed $v = \kappa$ on the low- and $v = -\lambda\kappa$ on the high-temperature isothermal stage, respectively. The established cyclic regime implies here, so that one has the distribution (51a) at the points “1” and “4” and (51b) at the points “2” and “3” of the cycle — there is no relaxation on the isentropes, as discussed before.

With (58) we get the following correction terms to the quasi-static heat and work along the isotherms $1 \rightarrow 2$ and $3 \rightarrow 4$; respectively:

$$\begin{aligned} q_{12} &= \kappa\tau_R T_c \sum \epsilon_i \left(p_i^{(2)} - p_i^{(1)} \right) < 0; \\ q'_{12} &= -\alpha_1 T_c \sum \epsilon_i \left(p_i^{(1)} - \tilde{p}_i(\alpha_1) \right) > 0; \\ q''_{12} &= \alpha_2 T_c \sum \epsilon_i \left(p_i^{(2)} - \tilde{p}_i(\alpha_2) \right) > 0; \\ q_{34} &= \lambda(T_h/T_c) q_{12} < 0; \\ q'_{34} &= -(T_h/T_c) q''_{12} < 0; \\ q''_{34} &= -(T_h/T_c) q'_{12} < 0; \\ w_{12} &= -q_{12} > 0; \\ w_{34} &= -q_{34} > 0. \end{aligned} \quad (61)$$

Eq. (59b) yields the correction to the quasi-static work along the isentropes $2 \rightarrow 3$ and $4 \rightarrow 1$, respectively:

$$\begin{aligned} w'_{23} &= \alpha_2 \Delta T \sum \epsilon_i \left(p_i^{(2)} - \tilde{p}_i(\alpha_2) \right) > 0; \\ w'_{41} &= -\alpha_1 \Delta T \sum \epsilon_i \left(p_i^{(1)} - \tilde{p}_i(\alpha_1) \right) > 0; \end{aligned} \quad (62)$$

Here we have observed $\Delta g(\gamma) = \alpha \Delta T$, which follows from (15) and (17).

The inequalities (sign) in (61) and (62) are proven in Appendix B. The sign of every correction term remains the same for any κ and λ , allowing us to sketch their general scheme in Fig. 5. Of course, all the terms listed here relate to the corresponding cycle step as a whole, not allowing any physical separation. Nevertheless, such a representation proves to be useful for the purpose of the heat and work transfer analysis, being performed at various driving speed regimes as well as in comparison with the cycles of other kinds.

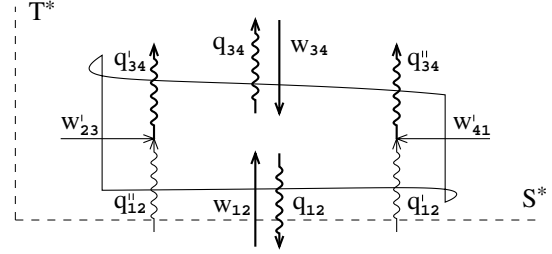


Fig. 5. Corrections (61) and (62) to the quasi-static heat and work along the stages of Carnot-like machine cycle (Fig. 4). Straight lines denote work, wavy ones – heat. Arrows pointing into the contour indicate energy flows into the system. (The primary, quasi-static contributions (21) and (22) providing the machine action are not shown.)

In the limit of very slow driving, $(\kappa\tau_R/\Delta\alpha) \ll 1$, one has (see App. C):

$$\begin{aligned} p_i^{(2)} - p_i^{(1)} &= \tilde{p}_i(\alpha_2) - \tilde{p}_i(\alpha_1) + \mathcal{O}[\kappa\tau_R], \\ p_i^{(1)} - \tilde{p}_i(\alpha_1) &= \lambda\kappa\tau_R \left(\frac{d\tilde{p}_i}{d\alpha} \right)_{\alpha_1} + o[\kappa\tau_R], \\ p_i^{(2)} - \tilde{p}_i(\alpha_2) &= -\kappa\tau_R \left(\frac{d\tilde{p}_i}{d\alpha} \right)_{\alpha_2} + o[\kappa\tau_R]; \end{aligned} \quad (63)$$

which means that all the terms in (61) and (62) are of first order in $\kappa\tau_R$. In Sec. 5.4 these results will be used in order to reveal the fast degradation of the machine efficiency with increasing driving speed κ .

In the limit of very fast driving, $(\Delta\alpha/\kappa\tau_R) \ll 1$, the terms above can be shown to be (App. C):

$$\begin{aligned} p_i^{(2)} - p_i^{(1)} &= -\frac{\Delta\alpha}{\lambda(\kappa\tau_R)^2} \cdot \mathcal{I}_i + o\left[\left(\frac{\Delta\alpha}{\kappa\tau_R}\right)^2\right], \\ p_i^{(1;2)} - \tilde{p}_i(\alpha_{1;2}) &= \bar{p}_i - \tilde{p}_i(\alpha_{1;2}) + \frac{1-\lambda}{\lambda\kappa\tau_R} \cdot \mathcal{I}_i + o\left[\frac{\Delta\alpha}{\kappa\tau_R}\right]; \end{aligned} \quad (64)$$

where

$$\begin{aligned} \mathcal{I}_i &:= \frac{1}{\Delta\alpha} \int_{\alpha_1}^{\alpha_2} (\bar{p}_i - \tilde{p}_i(\alpha)) \alpha d\alpha, \\ \bar{p}_i &:= \frac{1}{\Delta\alpha} \int_{\alpha_1}^{\alpha_2} \tilde{p}_i(\alpha) d\alpha; \end{aligned} \quad (65)$$

– the latter being the average of $\tilde{p}_i(\alpha)$ over the interval $[\alpha_1; \alpha_2]$.

The result (64) supports the intuitive expectation for the collapse of the cycle on (S^*, T^*) -space (Fig. 4) at high driving speed κ . The only energy flows surviving $\kappa\tau_R \rightarrow \infty$ are the total work along the isentropic stages, $W_{23;41}^*$, and the quasi-static part of the work along the isotherms:

$$\begin{aligned} W_{23;41}^* &= \pm \Delta T \alpha_{2;1} \sum \epsilon_i \bar{p}_i; \\ W_{12;34} &= \pm T_{c;h} \Delta\alpha \sum \epsilon_i \bar{p}_i. \end{aligned} \quad (66)$$

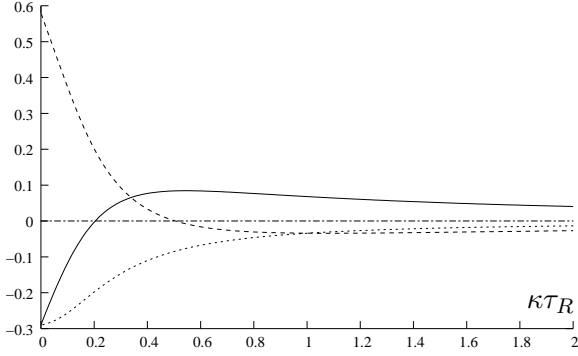


Fig. 6. Behaviour of W^* (solid lines), Q_{34}^* (dashed lines) and Q_{12}^* (dotted lines) with increasing velocity for a Carnot cycle performed by a four level system. The chosen parameters are $\{\epsilon_i\}_{i=1}^N = \{-3/2; -1/2; 1/2; 3/2\}$ and $\alpha_1 = 0.2$, $\alpha_2 = 0.8$, $T_c = 1$, $T_h = 2$. As one can see, both W and Q_{34}^* change their sign at certain velocities, while Q_{12}^* always stays negative.

The heat flows Q^* in the limit $(\Delta\alpha/\kappa\tau_R) \ll 1$ are:

$$\begin{aligned} Q_{12}^* &= -T_c \frac{\Delta\alpha}{\kappa\tau_R} \sum \epsilon_i \mathcal{I}_i + o\left[\frac{\Delta\alpha}{\kappa\tau_R}\right]; \\ Q_{34}^* &= -T_h \frac{\Delta\alpha}{\lambda\kappa\tau_R} \sum \epsilon_i \mathcal{I}_i + o\left[\frac{\Delta\alpha}{\kappa\tau_R}\right], \end{aligned} \quad (67)$$

negative on the both isothermal stages (App. B). Sure, there is no machine action left at $\kappa\tau_R \gg 1$.

A comment must be made concerning the scheme in Fig. 5. The triples $(\mathbf{q}'_{12}; \mathbf{w}'_{41}; \mathbf{q}''_{34})$ and $(\mathbf{q}''_{12}; \mathbf{w}'_{23}; \mathbf{q}'_{34})$ look like effective heat-pumps, counteracting the primary machine action along the cycle. This impression is supported by the balance relations, following from (61) and (62):

$$\begin{aligned} \mathbf{q}'_{12} + \mathbf{w}'_{41} + \mathbf{q}''_{34} &= 0; \\ \mathbf{q}''_{12} + \mathbf{w}'_{23} + \mathbf{q}'_{34} &= 0, \end{aligned} \quad (68)$$

and may insinuate the idea of a change-over to a heat pump at some values of κ and λ . As a matter of fact, this never happens for a cycle of the kind under consideration; it is proven in App. D, that $Q_{12}^* < 0$ always holds — there is no heat absorption from the cold bath as a complete result of the low-temperature isothermal step of the cycle.

To conclude this chapter, we want to briefly discuss how the Carnot cycle converts from working as a heat engine to its final state at high velocity, described before. Fig. 6 shows the development of work and heat for increasing driving velocity. The value of the velocities on which W^* and Q_{34}^* change their signs depends on the chosen parameters. However, this behaviour, as such, is typical for the Carnot cycle and can schematically be illustrated as in Fig. 7.

5.4 The efficiency at maximum power output

In the following we restrict ourselves to corrections to the quasi-static heat and work along the cycle stages linear in

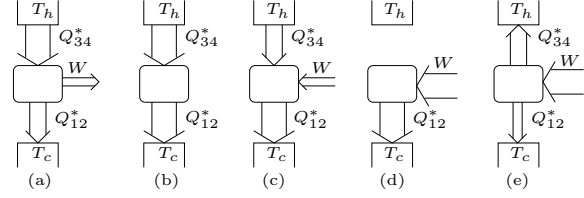


Fig. 7. The development of the Carnot cycle can be divided into five steps: For small $\kappa\tau_R$, the cycle works as a heat engine (a). At a certain velocity, the total work vanishes, and there is only heat flowing from the hot to the cold bath (b). After that point, work has changed its sign (c). Then there exists a velocity, where Q_{34}^* vanishes. The work therefore is completely transformed into heat, flowing into the cold bath (d). Finally, heat is flowing in the cold as well as in the hot bath (e), which corresponds to the high driving speed limit, discussed before. Note, that the size of the arrows is rescaled at each picture: Of course all components of heat and work decrease for increasing velocity as stated before.

the driving speed. In the appropriate limit (63) eqs. (61–62) result in

$$\begin{aligned} \{\mathbf{w}_{12}; \mathbf{w}_{34}\} &= \{-\mathbf{q}_{12}; -\mathbf{q}_{34}\} = \{T_c; \lambda T_h\} \times \kappa\tau_R a, \\ \text{where } a &:= \sum \epsilon_i (\tilde{p}_i(\alpha_1) - \tilde{p}_i(\alpha_2)) > 0; \end{aligned} \quad (69a)$$

$$\begin{aligned} \{\mathbf{q}'_{12}; \mathbf{w}'_{41}; \mathbf{q}''_{34}\} &= \{T_c; \Delta T; -T_h\} \times \lambda\kappa\tau_R b', \\ \text{where } b' &:= \alpha_1 \sum \epsilon_i (-d\tilde{p}_i/d\alpha)_{\alpha_1} > 0; \end{aligned} \quad (69b)$$

$$\begin{aligned} \{\mathbf{q}''_{12}; \mathbf{w}'_{23}; \mathbf{q}'_{34}\} &= \{T_c; \Delta T; -T_h\} \times \kappa\tau_R b'', \\ \text{where } b'' &:= \alpha_2 \sum \epsilon_i (-d\tilde{p}_i/d\alpha)_{\alpha_2} > 0. \end{aligned} \quad (69c)$$

(The inequalities are proven in Appendix B.)

We assume, in addition, that the relative part of the time per cycle spent on isothermal steps remains always the same, say δ . Hence, the period Δt for one full cycle turns out to be [21]:

$$\Delta t = \frac{\Delta\alpha}{\delta\kappa} \frac{\lambda + 1}{\lambda}. \quad (70)$$

The ratio of the total work output per full cycle, W^* , to the heat, $Q_{T_h}^*$, absorbed on the high-temperature isothermal step, yields the efficiency η^* . As follows from the scheme on Fig. 5 and (69), one gets:

$$\eta^* = \frac{W - \kappa\tau_R((T_c + \lambda T_h)a + \lambda\Delta T b' + \Delta T b'')}{Q_{T_h} - \kappa\tau_R T_h(\lambda(a + b') + b'')} \quad (71)$$

One easily convinces oneself that this result is bounded from above by the quasi-static Carnot limit

$$\frac{W}{Q_{T_h}} = \eta^c = \frac{\Delta T}{T_h}, \quad (72)$$

reached at $\kappa = 0$. The power output $\mathcal{P}^* = W^*/\Delta t$ is given by

$$\begin{aligned} \mathcal{P}^* &= \frac{\delta\kappa\lambda}{\Delta\alpha(\lambda + 1)} \\ &\times \left(W - \kappa\tau_R((T_c + \lambda T_h)a + \lambda\Delta T b' + \Delta T b'') \right) \end{aligned} \quad (73)$$

which confirms that $\mathcal{P}^* = 0$ for $\kappa = 0$, i.e. for the maximum Carnot efficiency η^C .

Our aim now is to maximize \mathcal{P}^* with respect to parameters κ and λ and to find the corresponding thermodynamic efficiency (71).

The condition for an extremum, $\partial_\kappa \mathcal{P}^* = \partial_\lambda \mathcal{P}^* = 0$, yields

$$\begin{cases} W = 2\kappa\tau_R((T_c + \lambda T_h)a + \lambda\Delta T b' + \Delta T b''), \\ W = \kappa\tau_R((T_c + \lambda T_h)a + \lambda\Delta T b' + \Delta T b'') \\ + \kappa\tau_R\lambda(\lambda + 1)(T_h a + \Delta T b'). \end{cases} \quad (74)$$

It follows from (74), that the maximum of \mathcal{P}^* occurs at:

$$\lambda^2 = \frac{T_c}{T_h} \cdot \frac{1 + \Delta T b''/T_c a}{1 + \Delta T b'/T_h a}. \quad (75)$$

Eliminating now $Q_{\mathcal{T}_h}$, W and λ in (71) by means of (72) and those maximum conditions, one obtains:

$$\eta_{max\mathcal{P}}^* = \eta^C \left(1 + \frac{1}{\sqrt{(1 + \frac{\Delta T b'}{T_h a})(1 + \frac{\Delta T b''}{T_c a})}} \sqrt{\frac{T_c}{T_h}} \right)^{-1}. \quad (76)$$

Only in the case, when $\Delta T b'/T_h a$ and $\Delta T b''/T_c a$ can be neglected, does this result reproduce the celebrated Curzon-Ahlborn efficiency [21, 29]:

$$\eta_{max\mathcal{P}}^* \approx \eta^{CA} = 1 - \sqrt{\frac{T_c}{T_h}}, \quad \text{if } \frac{\Delta T b'}{T_h a}, \frac{\Delta T b''}{T_c a} \ll 1. \quad (77)$$

But $\eta_{max\mathcal{P}}^*$ will be larger than this otherwise.

This discrepancy derives from those terms in the heat and work beyond the quasi-static limit, that may be regarded as a sort of *residual non-equilibrium effect*, namely, the triples $(\mathbf{q}'_{12}; \mathbf{w}'_{41}; \mathbf{q}''_{34})$ and $(\mathbf{q}''_{12}; \mathbf{w}'_{23}; \mathbf{q}'_{34})$ (69). In fact, they originate from the discrepancy between the steered attractor $\{\tilde{p}_i(\alpha)\}_{i=1}^N$ and the values of p_i (51) lagging behind at the cycle turning points. Spoiling the machine performance, they reduce at the same time the total heat $Q_{\mathcal{T}_h}$, absorbed per cycle from the high-temperature bath. Note, in the purely phenomenological thermodynamic setup by Curzon and Ahlborn [21] such an effect could not be envisaged: This model is a prime example for the so-called endoreversible approach to thermodynamic processes (cf. [2]).

In order to obtain, at least, a rough estimate for the terms $\Delta T b'/T_h a$ and $\Delta T b''/T_c a$, one can make use of Taylor's formula for $\tilde{p}_i(\alpha)$ in (69) to get, observing (17) and (15):

$$\frac{\Delta T b'}{T_h a} \approx \frac{(\Delta g)_{S_1}}{(\Delta g)_{\mathcal{T}_h}}; \quad \frac{\Delta T b''}{T_c a} \approx \frac{(\Delta g)_{S_2}}{(\Delta g)_{\mathcal{T}_c}}, \quad (78)$$

where $(\Delta g)_{\mathcal{T}_{c,h}}$ and $(\Delta g)_{S_{1,2}}$ stand for increments of function $g(\gamma)$ along the corresponding isotherms and isentropes.

It follows from (78), that one can expect Curzon-Ahlborn's result (77) in case of Carnot cycles (Fig. 1 and Fig. 2) with small enough ΔT and large enough $\Delta\alpha$ (eventually large enough ΔS). For our present model parameters, however, these conditions are obviously violated and the optimum η , indeed, lies between the Carnot and the Curzon-Ahlborn result, both for the exact and the linearized calculation (Fig. 8).

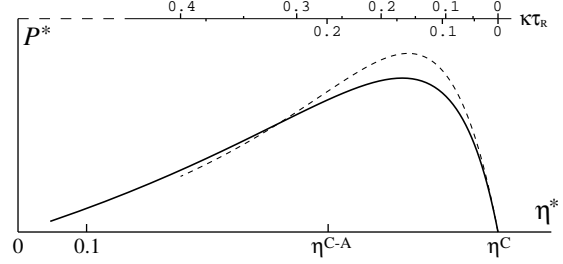


Fig. 8. Power output $\mathcal{P}^* = W^*/\Delta t$ (arbitrary units) vs. Efficiency $\eta^* = W^*/Q_{\mathcal{T}_h}^*$. The solid line and the lower $\kappa\tau_R$ -scale correspond to the linear driving speed approximation (71) and (73), at $\lambda = 0.756$ (75). The dashed line and the upper $\kappa\tau_R$ -scale correspond to exact calculations based on (51), when the maximal power output appears to be achieved at $\lambda = 1.040$.

5.5 Finite-time Otto cycle

We finally turn to the Otto machine cycle shown in Fig. 3, run now with finite driving speed. Again we allow for two different speeds on the isochors, in accordance with (50), and no bath coupling and no relaxation are assumed along the isentropes. The distributions p_i at the cycle's turning points “1” (“4”) and “2” (“3”) are then given by (51a) and (51b), respectively.

The heat and work along the cycle steps then follow from (59) and (60):

$$\begin{aligned} Q_{12}^* &= g(\gamma_1) \sum \epsilon_i (p_i^{(2)} - p_i^{(1)}) < 0, \\ W_{23}^* &= [g(\gamma_2) - g(\gamma_1)] \sum \epsilon_i p_i^{(2)}, \\ Q_{34}^* &= -g(\gamma_2) \sum \epsilon_i (p_i^{(2)} - p_i^{(1)}) > 0, \\ W_{41}^* &= -[g(\gamma_2) - g(\gamma_1)] \sum \epsilon_i p_i^{(1)}; \end{aligned} \quad (79)$$

the inequalities are proven in App. B.

The efficiency can now easily be calculated: With increasing $g(\gamma)$ we get

$$\eta^{*O} = \frac{-(W_{23}^* + W_{41}^*)}{Q_{34}^*} = 1 - \frac{g(\gamma_1)}{g(\gamma_2)} \quad (80)$$

With decreasing $g(\gamma)$, one has to run the cycle clockwise to achieve heat-engine performance, which results in the efficiency

$$\eta^{*O} = 1 - \frac{g(\gamma_2)}{g(\gamma_1)}, \quad (81)$$

i.e. exactly the same as in the quasi-static limit (30). So, the efficiency of the Otto cycle is independent of the driving speed. In particular, the efficiency does not depend on the power of the engine, which is totally different from the behaviour of the Carnot cycle discussed before. The constancy of the efficiency of course does not mean, that heat and work are constant too. All parts go to zero with increasing velocity, as shown in Fig. 9.

Fig. 10 shows a ST-diagram for an Otto cycle. In this diagram, one can also see the decrease of the work output

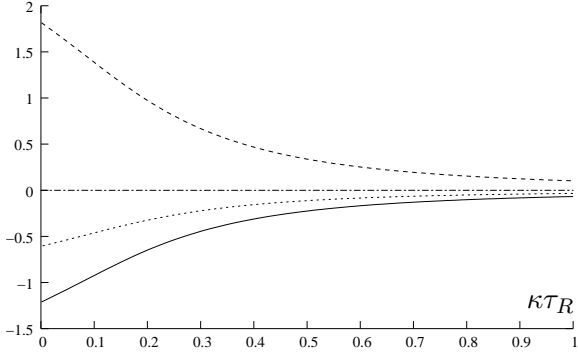


Fig. 9. Behaviour of W^* (solid lines), Q_{34}^* (dashed lines) and Q_{12}^* (dotted lines) with increasing velocity for an Otto cycle of a four level system. The chosen parameters are $\{\epsilon_i\}_{i=1}^N = \{-3/2; -1/2; 1/2; 3/2\}$ and $\alpha_1 = 0.2$, $\alpha_2 = 0.8$, $\gamma_1 = 1$, $\gamma_2 = 3$. As one can see, the ratio $\frac{W^*}{Q_{34}^*}$, which defines the efficiency always stays the same.

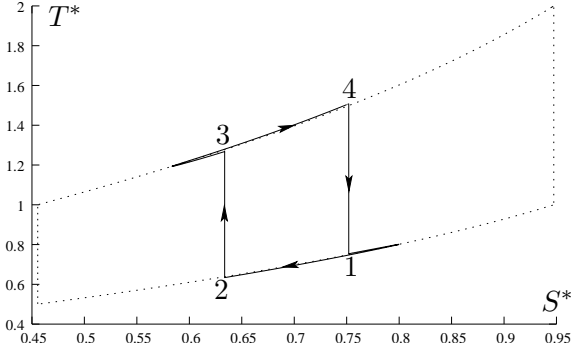


Fig. 10. ST-diagram for an Otto cycle of a four level system with $\{\epsilon_i\}_{i=1}^N = \{-3/2; -1/2; 1/2; 3/2\}$ and $\alpha_1 = 1$, $\alpha_2 = 2$, $\gamma_1 = 1$, $\gamma_2 = 2$. The dotted lines hold for the quasi-static limit, the solid lines for $\kappa\tau_R = 0.5$. The points 1 to 4 correspond to the points in Fig. 3.

per cycle for increasing speed, since the encircled area decreases. But in contrast to the Carnot cycle (Fig. 4), the finite speed does not cause any loops here.

6 Conclusions

We have considered a single quantum object with a discrete spectrum, an open system. The impact of its environment has been supposed to be reducible to a parametrized distortion of the spectrum and to a parametrized change of the state. The mean energy U and the von Neumann entropy S can then be written as unique functions of these controls. The same holds for any pertinent thermodynamic quantity including heat and work. We have noted that those quantities (except U and S) are connected with a process, not just a state. While there can be no operators underlying these quantities, they can, nevertheless, be defined for any appropriately embedded quantum system, even down to a single spin.

Thermodynamic machines arise, if a cycle is enforced on such a two-dimensional control space. The pertinent

efficiencies for two standard machine cycles have been obtained analytically and numerically. They all observe the Carnot limit, which has been identified to result from the interplay between mechanical and statistical control rather than from thermal equilibrium as such. Consequently, there is no way to violate the second law of thermodynamics, not even by using exotic attractor states.

Our approach is meant to be some kind of a minimal model capturing the essentials of any quantum thermodynamic machine: This is not a substitute for more detailed investigations; however, contrary to concrete models, we can here treat any type of cycle (Carnot, Otto, Stirling etc.) on equal footing — without specifying, though, by which physical means the control might be implemented.

While coherence has been excluded here, dynamical effects (finite process speed) have been included after defining an internal relaxation time scale. The resulting non-equilibrium features have been incorporated in terms of renormalized thermodynamic quantities. As has been shown, under such external control conditions even the concept of a process temperature should still be applicable.

The optimum condition for maximum power of a heat engine has been studied. The celebrated Curzon-Ahlborn limit can be obtained under appropriate conditions.

Many model types can easily, if in a formal way, be implemented: Different control functions, different dynamical features, different cycle types, different spectra.

A Carnot cycle for non-canonical attractor

A.1 Nearly-uniform distribution

As a specific attractor consider the nearly-uniform distribution $\{\tilde{p}_i(\alpha)\}_{i=1}^N$:

$$\tilde{p}_i(\alpha) = \begin{cases} 1 - \alpha, & i = 1; \\ \alpha/(N - 1), & i = 2 \dots N. \end{cases} \quad \alpha \in (0, 1) \quad (82)$$

The process temperature (8) in the quasi-static limit (3) can be written as

$$T = g(\gamma)\tilde{\epsilon} \ln^{-1} \frac{(N - 1)(1 - \alpha)}{\alpha}, \quad (83)$$

with $\tilde{\epsilon} := (N - 1)^{-1} \sum_{i=2}^N \epsilon_i - \epsilon_1$. From $\epsilon_1 < \epsilon_{(i>1)}$ it follows that $\tilde{\epsilon} > 0$, so the area of positive temperatures on the (α, γ) -plane is restricted by $\alpha < 1 - N^{-1}$.

The function Θ , that defines the shape of isothermal curves $g(\gamma) = T \cdot \Theta(\alpha)$, is now

$$\Theta_U(\alpha) = \tilde{\epsilon}^{-1} \ln \frac{(N - 1)(1 - \alpha)}{\alpha}; \quad (84)$$

and an example of the corresponding Carnot's cycle is sketched in Fig. 11.

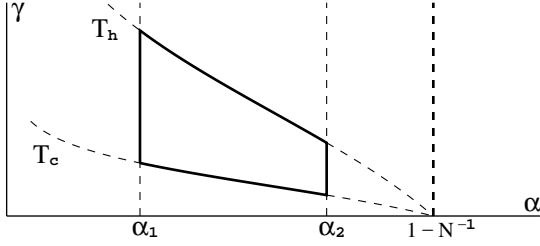


Fig. 11. Carnot cycle on the (α, γ) -plane associated with the nearly-uniform distribution (82) and $g(\gamma) = \gamma$. It is composed by segments of isentropes $\alpha = \alpha_{1,2}$ and isotherms $\gamma = T_{c,h} \cdot \Theta_U(\alpha)$ (84); ($T_h > T_c$).

A.2 Tsallis' distribution

The attractor $\{\tilde{p}_i(\alpha)\}_{i=1}^N$ is now taken to be the Tsallis' distribution [30]:

$$\begin{aligned} \tilde{p}_i(\alpha) &= Z_{\mathcal{T}_s}^{-1} \left(1 - \alpha(q-1)\epsilon_i\right)^{\frac{1}{q-1}}, \\ Z_{\mathcal{T}_s} &= \sum \left(1 - \alpha(q-1)\epsilon_i\right)^{\frac{1}{q-1}}; \end{aligned} \quad (85)$$

with the specific parameter q , bounded by $q \in (0, 2)$; at $q = 1$ the case reduces to the canonical one (16).

Introducing the mean value $\langle \cdot \rangle$ and the covariance $\langle\langle \cdot; \cdot \rangle\rangle$ in a standard way:

$$\langle f \rangle := \sum f_i \tilde{p}_i, \quad \langle\langle f; g \rangle\rangle := \langle fg \rangle - \langle f \rangle \langle g \rangle, \quad (86)$$

as well as an auxiliary variable

$$u_i(\alpha; q) = \frac{\alpha(q-1)\epsilon_i}{1 - \alpha(q-1)\epsilon_i}, \quad (87)$$

one can now express the isotherm shape function $\Theta_{\mathcal{T}_s}(\alpha; q)$, resulting from (8), as

$$\Theta_{\mathcal{T}_s}(\alpha; q) = \alpha \frac{\langle\langle u; \ln(1+u) \rangle\rangle}{\langle\langle u; u/(1+u) \rangle\rangle}. \quad (88)$$

Note, that $\ln(1+u)$ and $u/(1+u)$ are both increasing functions of u , therefore the RHS is always positive here.

An example of a Carnot cycle with isotherms of such a kind is sketched in Fig. 12. One can see that these isotherms are very similar to the canonical ones (cf. Fig. 1) as long as α is small enough. This is easily shown taking $\alpha\epsilon_i \ll 1$ for (88).

B Inequalities

Here we prove some inequalities concerning the heat and work flows in case of the canonical attractor (16). Considering the first derivative of $\tilde{p}_i(\alpha)$, one easily gets

$$\frac{d\tilde{p}_i(\alpha)}{d\alpha} = \sum_k (\epsilon_k - \epsilon_i) \tilde{p}_k(\alpha) \tilde{p}_i(\alpha) \quad (89)$$

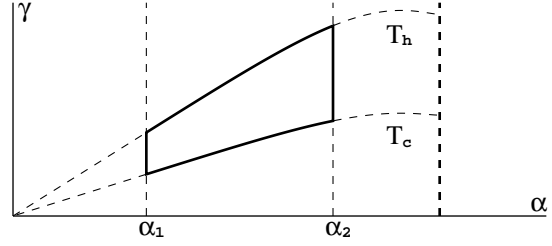


Fig. 12. Carnot cycle in the (α, γ) -plane associated with Tsallis' distribution (85) and $g(\gamma) = \gamma$ at $q = 1.4$ and $\{\epsilon_i\} = \{-3/2; -1/2; 1/2; 3/2\}$. The cycle is composed by segments of isentropes $\alpha = \alpha_{1,2}$ and isotherms $\gamma = T_{c,h} \cdot \Theta_{\mathcal{T}_s}(\alpha)$ (88); ($T_h > T_c$). Note, that the domain of definition for (85) is restricted by $\alpha < [\max_i (q-1)\epsilon_i]^{-1}$.

and, consequently:

$$\begin{aligned} \sum_{i=1}^N \epsilon_i \frac{d\tilde{p}_i}{d\alpha} &= Z_{Can}^{-2} \sum_{i,k=1}^N \epsilon_i (\epsilon_k - \epsilon_i) e^{-\alpha(\epsilon_k + \epsilon_i)} \\ &= -Z_{Can}^{-2} \sum_{i < k} (\epsilon_k - \epsilon_i)^2 e^{-\alpha(\epsilon_k + \epsilon_i)} < 0. \end{aligned}$$

This implies the following inequalities:

$$\sum \epsilon_i (\tilde{p}_i(\alpha_1) - \tilde{p}_i(\alpha_2)) > 0, \quad \text{if } \alpha_1 < \alpha_2; \quad (90)$$

$$\sum \epsilon_i (d\tilde{p}_i/d\alpha) < 0; \quad \sum \epsilon_i \int \alpha d\tilde{p}_i(\alpha) < 0. \quad (91)$$

Consider the terms $\sum \epsilon_i (p_i^{(1;2)} - \tilde{p}_i(\alpha_{1;2}))$ from (61), where the distributions $p_i^{(1;2)}$ at the cycle turning points are defined in (51). Integration by parts leads to:

$$\sum \epsilon_i (p_i^{(1;2)} - \tilde{p}_i(\alpha_{1;2})) = \pm \int_{\alpha_1}^{\alpha_2} \mathcal{F}_{1;2} \cdot \left(\sum \epsilon_i \frac{d\tilde{p}_i}{d\alpha} \right) \cdot d\alpha,$$

where

$$\mathcal{F}_{1;2} = \frac{\exp\{(\alpha - \alpha_{2;1})/\kappa\tau_R\} - \exp\{(\alpha_{2;1} - \alpha)/\lambda\kappa\tau_R\}}{\exp\{\mp\Delta\alpha/\kappa\tau_R\} - \exp\{\pm\Delta\alpha/\lambda\kappa\tau_R\}}.$$

Observing $\mathcal{F}_{1;2} > 0$ and the first inequality in (91), one comes up with:

$$\sum \epsilon_i (p_i^{(1;2)} - \tilde{p}_i(\alpha_{1;2})) \leq 0; \quad (92)$$

For the next inequality we need the following

Lemma: For any two monotone decreasing functions $f(x)$ and $h(x)$ the inequality $\int_a^b h(x)f(x)dx > 0$ follows from $\int_a^b h(x)dx = 0$.

Proof: Define $H(x) = \int_a^x h(x')dx'$ with the obvious property: $H(x) > H(a) = H(b) = 0$ for $a < x < b$. Applying

integration by parts, one gets:

$$\begin{aligned} \int_a^b h(x)f(x)dx &= [H(x)f(x)]_a^b - \int_a^b \frac{df}{dx}H(x)dx \\ &= - \int_a^b \frac{df}{dx}H(x)dx > 0, \end{aligned}$$

observing $(df/dx) < 0$ and $H(x) > 0$.

Consider now the term $\sum \epsilon_i (p_i^{(2)} - p_i^{(1)})$ which occurs in RHS of (61) and (79). With (51) it reduces to

$$\begin{aligned} \sum \epsilon_i (p_i^{(2)} - p_i^{(1)}) &= \frac{1}{\kappa\tau_R} \left\{ 1 - e^{-\frac{\Delta\alpha}{\kappa\tau_R} \frac{\lambda+1}{\lambda}} \right\}^{-1} \\ &\times \int_{\alpha_1}^{\alpha_2} h(\alpha') \left(\sum \epsilon_i \tilde{p}_i(\alpha') \right) d\alpha'; \end{aligned} \quad (93)$$

with

$$h(\alpha') = e^{-\frac{\alpha' - \alpha_1}{\kappa\tau_R}} \left(1 - e^{-\frac{\Delta\alpha}{\lambda\kappa\tau_R}} \right) + \frac{1}{\lambda} e^{-\frac{\alpha_2 - \alpha'}{\lambda\kappa\tau_R}} \left(e^{-\frac{\Delta\alpha}{\kappa\tau_R}} - 1 \right).$$

One can easily check that both $\int_{\alpha_1}^{\alpha_2} h(\alpha') d\alpha' = 0$ and $(dh/d\alpha') < 0$ hold. It follows from (91) that $\sum \epsilon_i \tilde{p}_i(\alpha')$ is a decreasing function of α' as well. The lemma proven above ensures the integral in (93) to be positive and consequently:

$$\sum \epsilon_i (p_i^{(2)} - p_i^{(1)}) < 0. \quad (94)$$

Consider, at last, the term $\sum \epsilon_i \mathcal{I}_i$ from (67). The integral \mathcal{I}_i is defined in (65) and reduces to:

$$\int_{\alpha_1}^{\alpha_2} (\bar{p}_i - \tilde{p}_i(\alpha)) \alpha d\alpha = \left(\int_{\alpha_1}^{\bar{\alpha}} + \int_{\bar{\alpha}}^{\alpha_2} \right) (\bar{\alpha} - \alpha) \tilde{p}_i(\alpha) d\alpha,$$

where $\bar{\alpha} = (\alpha_2 + \alpha_1)/2$. It follows from the mean-value theorem that

$$\begin{aligned} &\left(\int_{\alpha_1}^{\bar{\alpha}} + \int_{\bar{\alpha}}^{\alpha_2} \right) (\bar{\alpha} - \alpha) \left(\sum \epsilon_i \tilde{p}_i(\alpha) \right) d\alpha \\ &= \sum \epsilon_i \tilde{p}_i(\theta_1) \int_{\alpha_1}^{\bar{\alpha}} (\bar{\alpha} - \alpha) d\alpha \\ &+ \sum \epsilon_i \tilde{p}_i(\theta_2) \int_{\bar{\alpha}}^{\alpha_2} (\bar{\alpha} - \alpha) d\alpha \\ &= \sum \epsilon_i (\tilde{p}_i(\theta_1) - \tilde{p}_i(\theta_2)) \int_0^{\bar{\alpha}} u du, \end{aligned}$$

where $\alpha_1 < \theta_1 < \bar{\alpha} < \theta_2 < \alpha_2$. With (90) one gets:

$$\Delta\alpha \sum \epsilon_i \mathcal{I}_i = \sum \epsilon_i \int_{\alpha_1}^{\alpha_2} (\bar{p}_i - \tilde{p}_i(\alpha)) \alpha d\alpha > 0. \quad (95)$$

C Asymptotes

To get the asymptotic solution of the relaxation equation (48) in the slow driving limit $(v\tau_R/\Delta\alpha) \ll 1$, we

start an iterative procedure: For this purpose we rewrite (48) as

$$p_i = \tilde{p}_i(\alpha) - v\tau_R (dp_i/d\alpha); \quad (96)$$

The zeroth approximation is given by $p_i \approx \tilde{p}_i(\alpha)$. The first order is obtained by the corresponding substitution on the right hand side of (96):

$$p_i \approx \tilde{p}_i - v\tau_R (d\tilde{p}_i/d\alpha). \quad (97)$$

This result, in turn, will be used, in the next iteration step:

$$p_i \approx \tilde{p}_i - v\tau_R (d\tilde{p}_i/d\alpha) + (v\tau_R)^2 (d^2\tilde{p}_i/d\alpha^2), \quad (98)$$

and so on.

Consider now the asymptotes for the distributions $p_i^{(1;2)}$ at the cycle's turning points (51), first, in the limit of very slow driving, here $(\kappa\tau_R/\Delta\alpha) \ll 1$. Both $p_i^{(1)}$ and $p_i^{(2)}$ can be regarded as particular solutions of Eq. (96) obtained at the specially chosen parameters and initial values. So, $p_i^{(1)}$ is achieved at $\alpha = \alpha_1$ through the evolution with $v = -\lambda\kappa$ and $\alpha_0 = \alpha_2$ (50) started at $p_i^{(0)} = p_i^{(2)}$. With (98) one gets:

$$p_i^{(1)} = \tilde{p}_i(\alpha_1) + \lambda\kappa\tau_R \left(\frac{d\tilde{p}_i}{d\alpha} \right)_{\alpha_1} + o[\kappa\tau_R]; \quad (99)$$

Treating in the same way $p_i^{(2)}$, one comes up with:

$$p_i^{(2)} = \tilde{p}_i(\alpha_2) - \kappa\tau_R \left(\frac{d\tilde{p}_i}{d\alpha} \right)_{\alpha_2} + o[\kappa\tau_R]; \quad (100)$$

In the limit of very fast driving, $(\Delta\alpha/\kappa\tau_R) \ll 1$, one has to expand the exponents contained on the RHS of (51) into power series. Collecting terms up to first order in $\frac{\Delta\alpha}{\kappa\tau_R}$ yields the results for $p^{(1;2)}$ presented in Eq. (64). Their difference, $(p^{(2)} - p^{(1)})$, however, turns out to be of the second order and needs the adequate accuracy in the treatment.

D Proof for $Q_{12}^* < 0$

In the stationary cyclic regime the system state evolution on the low-temperature stage $1 \rightarrow 2$ is given by Eq. (49) taken with $v = \kappa$, $\alpha_0 = \alpha_1$ and $p_i^{(0)} = p_i^{(1)}$. Let us denote this particular solution of the relaxation equation (48) as p_i^* ; its boundary values prove to be $p_i^*(\alpha_{1;2}) = p_i^{(1;2)}$ from (51). Consider the derivative of the sum $\sum \epsilon_i p_i^*$ as a function $\varphi(\alpha)$:

$$\varphi(\alpha) := \frac{d}{d\alpha} \sum \epsilon_i p_i^* = -(\kappa\tau_R)^{-1} \sum \epsilon_i (p_i^* - \tilde{p}_i(\alpha)),$$

applying (48).

It follows from (92) that the boundary values of $\varphi(\alpha)$ turn out to be $\varphi(\alpha_{1;2}) \geq 0$, so there must be at least one $\alpha^* \in (\alpha_1; \alpha_2)$ such that $\varphi(\alpha^*) = 0$ and, consequently,

$$\sum \epsilon_i p_i^*(\alpha^*) = \sum \epsilon_i \tilde{p}_i(\alpha^*).$$

Choosing α^* as a new initial point for (49), one can employ this equality in order to recast $\sum \epsilon_i p_i^*$ and then $\varphi(\alpha)$ into the new form:

$$\begin{aligned} \sum \epsilon_i p_i^* &= \sum \epsilon_i \tilde{p}_i(\alpha^*) e^{-\frac{\alpha-\alpha^*}{\kappa\tau_R}} \\ &+ (\kappa\tau_R)^{-1} \int_{\alpha^*}^{\alpha} \left(\sum \epsilon_i \tilde{p}_i(\alpha') \right) e^{-\frac{\alpha-\alpha'}{\kappa\tau_R}} d\alpha' \\ &= \sum \epsilon_i \tilde{p}_i(\alpha) - \int_{\alpha^*}^{\alpha} e^{-\frac{\alpha-\alpha'}{\kappa\tau_R}} d \left(\sum \epsilon_i \tilde{p}_i \right); \\ \varphi(\alpha) &= (\kappa\tau_R)^{-1} \int_{\alpha^*}^{\alpha} e^{-\frac{\alpha-\alpha'}{\kappa\tau_R}} d \left(\sum \epsilon_i \tilde{p}_i \right). \end{aligned}$$

With the first inequality in (91) it is clear now that

$$\varphi(\alpha) \geq 0 \quad \text{for } \alpha \leq \alpha^*, \quad (101)$$

so α^* introduced above is unique.

Consider now the integral originated from (40)

$$\int_{\alpha_1}^{\alpha_2} \alpha d \left(\sum \epsilon_i p_i^* \right) = \int_{\alpha_1}^{\alpha_2} \alpha \varphi(\alpha') d\alpha,$$

which yields the total heat exchange Q_{12}^* on the low-temperature isotherm $g(\gamma) = \alpha T_1$ of the Carnot cycle. It is convenient to split the interval of integration by α^* so that the mean-value theorem becomes employable:

$$\begin{aligned} \left(\int_{\alpha_1}^{\alpha^*} + \int_{\alpha^*}^{\alpha_2} \right) \alpha \varphi(\alpha) d\alpha &= \theta_1 \int_{\alpha_1}^{\alpha^*} \varphi(\alpha) d\alpha \\ &+ \theta_2 \int_{\alpha^*}^{\alpha_2} \varphi(\alpha) d\alpha, \end{aligned}$$

where $\alpha_1 < \theta_1 < \alpha^* < \theta_2 < \alpha_2$. According to (101), the first addend here is positive while the second one is negative. One estimates further:

$$\begin{aligned} &(\theta_1 \cdot \int_{\alpha_1}^{\alpha^*} + \theta_2 \cdot \int_{\alpha^*}^{\alpha_2}) \varphi(\alpha) d\alpha \\ &< \theta_2 \int_{\alpha_1}^{\alpha_2} \varphi(\alpha) d\alpha = \theta_2 \int_{\alpha_1}^{\alpha_2} d \left(\sum \epsilon_i p_i^* \right) \\ &= \theta_2 \sum \epsilon_i \left(p_i^{(2)} - p_i^{(1)} \right) < 0, \end{aligned}$$

as it follows from (94).

This completes the proof for

$$Q_{12}^* = \int_{\alpha_1}^{\alpha_2} \alpha d \left(\sum \epsilon_i p_i^* \right) < 0. \quad (102)$$

One of us (J. B.) gratefully acknowledges financial and other support from DAAD and the Russian Ministry for Education and Science in the framework of joint program ‘‘Michail Lomonosov’’. We thank Markus Henrich, Florian Rempp, and Georg Reuther for valuable discussions.

References

1. M.A. Nielsen, I.L. Chuang, *Quantum Computation and Quantum Information* (Cambridge U. P., 2000)
2. A. Bejan, *Advanced Engineering Thermodynamics* (Wiley, N.Y., 1988)
3. C. Truesdell, S. Bharatha, *Classical Thermodynamics as a Theory of Heat Engines* (Springer, New York, Berlin, 1977)
4. M. Toda, R. Kubo, N. Saito, *Statistical Physics I* (Springer Berlin, New York, 1983)
5. J. Gemmer, M. Michel, G. Mahler, *Quantum Thermodynamics* (Springer, 2004)
6. R.V. Chamberlain, *Science* **298**, 1172 (2002)
7. T.L. Hill, *Nano Letters* **1**, 111 (2001)
8. M. Michel, J. Gemmer, G. Mahler, *Int'l J. Mod. Phys. B* **20**, 4855 (2006)
9. R. Alicki, *J. Phys. A* **12**, L 103 (1979)
10. T. Feldmann, R. Kosloff, *Phys. Rev. E* **68**, 016101 (2003)
11. E. Geva, R. Kosloff, *J. Chem. Phys.* **97**, 4398 (1992)
12. M. Henrich, G. Mahler, M. Michel, *Phys. Rev. E* (in press 2007)
13. M. Henrich, M. Michel, G. Mahler, *Europhys. Lett.* **76**, 1058 (2006)
14. J.P. Palao, R. Kosloff, J. Gordon, *Phys. Rev. E* **64**, 056130 (2001)
15. H.T. Quan, P. Zhang, C.P. Sun, *Phys. Rev. E* **73**, 036122 (2006)
16. H.E.D. Scovil, E.O. Schulz-Du Bois, *Phys. Rev. Lett.* **2**, 262 (1959)
17. D. Segal, A. Nitzan, *Phys. Rev. E* **73**, 026109 (2006)
18. F. Tonner, G. Mahler, *Phys. Rev. E* **72**, 066118 (2005)
19. L. Hackermüller, K. Hornberger, *Nature* **427**, 711 (2004)
20. T. Jahnke, J. Birjukov, G. Mahler, *Eur. Phys. J. ST* (conference proceedings), (to be published)
21. F.L. Curzon, B. Ahlborn, *Am. J. Phys.* **43**, 22 (1975)
22. D.P. Sheehan, *AIP Conf. Proc.* (AIP Press, Melville, N.Y.) **643** (2002)
23. R. Jones, www.softmachines.org/wordpress/?p=127
24. T.P. Cheng, *Relativity, Gravitation and Cosmology* (Oxford U. P., 2005)
25. F. Rempp, M. Michel, G. Mahler, *Phys. Rev. A* (submitted 2007)
26. T.D. Kieu, *Phys. Rev. Lett.* **93**, 140403 (2004)
27. C.M. Bender, D.C. Brody, B.K. Meister, *Proc. Royal Soc. (London)* **A 458**, 1519 (2002)
28. F. Ritort, *cond-mat/0401311* (2004)
29. C.V.d. Broeck, *Phys. Rev. Lett.* **95**(19), 190602 (2005)
30. C. Tsallis, *J. Stat. Phys.* **52**, 169 (1988)